Real-time gene expression analysis in human xenografts for evaluation of histone deacetylase inhibitors

Ann Beliën,[1] Stefanie De Schepper,[4] Wim Floren,[1] Boud Janssens,[1] Ann Mariën,[1] Peter King,[1] Jacky Van Dun,[1] Luc Andries,[4] Jan Voeten,[2] Luc Bijnens,[3] Michel Janicot,[1] and Janine Arts[1]

[1]Oncology Discovery Research and Early Development, [2]Global Information Solutions, and [3]Nonclinical Biostatistics, Johnson & Johnson Pharmaceutical Research and Development, Beerse, Belgium; and [4]HistoGenex, Edegem, Belgium

Abstract

Real-time analysis of gene expression in experimental tumor models represents a major tool to document disease biology and evaluate disease treatment. However, monitoring gene regulation *in vivo* still is an emerging field, and thus far it has not been linked to long-term tumor growth and disease outcome. In this report, we describe the development and validation of a fluorescence-based gene expression model driven by the promoter of the cyclin-dependent kinase inhibitor $p21^{waf1,cip1}$. The latter is a key regulator of tumor cell proliferation and a major determinant in the response to many anticancer agents such as histone deacetylase inhibitors. In response to histone deacetylase inhibitors, induction of fluorescence in A2780 ovarian tumors could be monitored in living mice in a noninvasive real-time manner using whole-body imaging. Single p.o. administration of the histone deacetylase inhibitor MS-275 significantly induces tumor fluorescence in a time- and dose-dependent manner, which accurately predicted long-term antitumoral efficacy in individual mice following extended treatment. These findings illustrate that this technology allows monitoring of the biological response induced by treatment with histone deacetylase inhibitors. In addition to providing experimental pharmacokinetic/pharmacodynamic markers for investigational drugs, this model provides insight into the kinetics of *in vivo* regulation of transcription, which plays a key role in causing and maintaining the uncontrolled proliferation of tumor tissue. [Mol Cancer Ther 2006;5(9):2317–23]

Introduction

Transcriptional regulators are frequently altered in tumors and play a causal role in maintaining malignant phenotype (1). A well-known example is the tumor suppressor p53, which controls cellular response to radiation and chemotherapeutic agents and is inactivated in the majority of human tumors (2, 3). One of the main target genes of p53 is the cyclin-dependent kinase inhibitor $p21^{waf1,cip1}$, which is crucial for G_1 checkpoint control and for maintaining the G_2 checkpoint in response to DNA damage (4–7). In addition, $p21^{waf1,cip1}$ protein plays an important role in cell senescence and differentiation (8). $p21^{waf1,cip1}$ is highly regulated at the transcriptional level and its expression is induced by a broad panel of upstream signaling pathways. p53 activates $p21^{waf1,cip1}$ transcription through direct binding to Sp1, a constitutive transcriptional activator that binds to the GC-boxes in the proximal region of the $p21^{waf1,cip1}$ promoter. p53 binding results in the dissociation of histone deacetylase 1 (HDAC1), which is responsible for the constitutive suppression of the $p21^{waf1,cip1}$ gene (9). Histone deacetylase–induced transcriptional silencing is a key process in tumor growth (10) and several histone deacetylase inhibitors have shown promising activity in early clinical development (11).

As $p21^{waf1,cip1}$ is regulated by a large number of signaling pathways and is also a key determinant in the biological outcome after triggering these signaling pathways, an experimental model visualizing $p21^{waf1,cip1}$ gene expression in a real-time manner would be of value in predicting the long-term antitumor effect of investigational agents. In addition, such a model would allow rapid identification of novel antineoplastic agents in general, a process that is currently hampered by the limited throughput of mouse xenograft tumor studies, requiring long-term studies and the necessity for extensive compound synthesis. For this reason, many promising early compounds are not evaluated *in vivo* and potentially numerous promising new therapeutic agents are abandoned.

We have developed an experimental tumor model that allows noninvasive real-time analysis of signal transduction and gene expression in nude mice bearing human xenografts using whole-body imaging technology (12). Human A2780 ovarian carcinoma cells have been engineered with a reporter gene construct encoding the fluorescent ZsGreen protein, of which the expression is under the control of the $p21^{waf1,cip1}$ promoter. When s.c. grafted to athymic nude mice, A2780-$p21^{waf1,cip1}$ ZsGreen

Received 2/28/06; revised 6/16/06; accepted 6/29/06.

The costs of publication of this article were defrayed in part by the payment of page charges. This article must therefore be hereby marked advertisement in accordance with 18 U.S.C. Section 1734 solely to indicate this fact.

Requests for reprints: Janine Arts, Oncology Discovery Research and Early Development, Johnson & Johnson Pharmaceutical Research and Development, Turnhoutseweg 30, 2340 Beerse, Belgium.
Phone: 32-14-606325; Fax: 32-14-605403.
E-mail: jarts@prdbe.jnj.com

doi:10.1158/1535-7163.MCT-06-0112

ovarian xenografts allow noninvasive real-time imaging of gene expression regulation in living tumor-bearing mice. ZsGreen fluorescence fully parallels regulation of the endogenous $p21^{waf1,cip1}$ protein, and induction of fluorescence *in vivo* was found to accurately predict long-term antitumor activity of the HDAC inhibitor MS-275 in individual mice. Induction of the $p21^{waf1,cip1}$ promoter *in vivo* was observed in both the center and periphery of the experimental tumors, indicating an exposure and biological response in the entire tumor. Our data therefore show that this model allows the analysis of the mechanism of action of a selected drug *in vivo* and noninvasive real-time evaluation of the pharmacodynamic response to HDAC inhibitors in animal models.

Materials and Methods

Materials

Human A2780 ovarian carcinoma cells (American Type Culture Collection, Manassas, VA) were maintained as monolayers in RPMI 1640 supplemented with 10% FCS, 2 mmol/L L-glutamine, and gentamicin at 37°C in a humidified 5% CO_2 incubator. All cell culture reagents were purchased from Life Technologies, Inc. (Gaithersburg, MD). Trichostatin A was obtained from Calbiochem (San Diego, CA). Cell proliferation was measured by a classic 3-(4,5-dimethyl-2-thiazolyl)-2,5-diphenyl-2*H*-tetrazolium bromide assay (Serva, Heidelberg, Germany).

Production of the 1,300-kb $p21^{waf1,cip1}$ Promoter-ZsGreen Construct

To generate an HDAC inhibitor–responsive $p21^{waf1,cip1}$ promoter construct, genomic DNA was extracted from A2780 cells and used as template for nested PCR isolation of a 1.3-kb fragment containing the −1,300 to +88 region of the $p21^{waf1,cip1}$ promoter relative to the TATA box. The first amplification was done with the oligonucleotide pair GAGGGCGCGGTGCTTGG and TGCCGCCGCTCTCT-CACC. The resulting 4.5-kb fragment was reamplified with the oligos TCGGGTACCGAGGGCGCGGTGCTTGG and ATACTCGAGTGCCGCCGCTCTCTCACC and subsequently with the oligos TCGGGTACCGGTAGATGG-GAGCGGATAGACACATC and ATACTCGAGTGCCGC-CGCTCTCTCACC. The luciferase reporter was removed from the pGL3-basic plasmid (Promega, Leiden, the Netherlands) and replaced by the ZsGreen reporter (pZsGreen1-N1 plasmid, Clontech, Mountain View, CA) at *Kpn*I and *Xba*I restriction sites. pGL3-basic-ZsGreen-1300 was constructed via insertion of the above-mentioned 1.3-kb fragment of the human $p21^{waf1,cip1}$ promoter region into pGL3-basic-ZsGreen at the *Xho*I and *Kpn*I sites. All restriction enzymes were purchased from Boehringer Mannheim (Mannheim, Germany).

Generation of Stable Cell Lines

A2780 cells were seeded at a density of 2×10^5 per 10-cm diameter cell culture dish, grown for 24 hours, and transfected with 2 μg of pGL3-basic-ZsGreen-1300 and 0.2 μg of pSV2neo resistance vector using Lipofectamine 2000 (Invitrogen, Brussels, Belgium). Single-cell clones were obtained in medium containing G418 (450 μg/mL) and tested for detectable basal level of fluorescence to allow for detection of tumor mass in the absence of stimulation. All further studies were done with A2780-$p21^{waf1,cip1}$ZsGreen clone 5 (A2780-$p21^{waf1,cip1}$ZsGreen).

Fluorescence Detection of $p21^{waf1,cip1}$ Promoter Activity in Cell-Based Assays

A2780-$p21^{waf1,cip1}$ZsGreen cells were seeded at 10,000 per well into 96-well multititer plates, grown for 24 hours, and treated for an additional 24 hours with the indicated HDAC inhibitors. Subsequently, cells were fixed with 4% paraformaldehyde for 30 minutes and counterstained with Hoechst dye. $p21^{waf1,cip1}$ promoter activation leading to ZsGreen protein production (and thus fluorescence signal) was monitored by the Ascent Fluoroskan (Thermo Labsystems, Brussels, Belgium) by fluorescence-activated cell sorting or with a fluorescent microscope [Axiovert 135 (Zeiss, Jena, Germany), equipped with a green fluorescence (excitation, 450–490 nm; emission, 510 nm) filter set, supported by MagnaFire software (Optronics, Goleta, CA)]. Ascent Fluoroskan data are presented as mean ± variation of two independent experiments. IC_{50} values were calculated by nonlinear regression analysis using SigmaPlot 4.01 software. For fluorescence-activated cell sorting analysis of fluorescence, A2780-$p21^{waf1,cip1}$ZsGreen cells were seeded at a density of 3×10^5 per well in a six-well cell culture plate. Cells were treated with DMSO or 10^{-7} mol/L trichostatin A. After 24 hours, cells were collected and resuspended in 0.5-mL CellScrub Buffer (Gene Therapy Systems, Inc., San Diego, CA) at 4°C. Cells were subsequently analyzed on a FACScan (BD Biosciences, Erembodegem, Belgium) for ZsGreen fluorescence (detection filter set at 530 nm). Cell aggregates were filtered out and 10,000 events were analyzed. The effect of HDAC inhibitors on endogenous $p21^{waf1,cip1}$ protein expression was measured with a WAF1 ELISA (Oncogene, Cambridge, MA) according to the prescription of the manufacturer. Data are presented as mean ± variation of two independent experiments.

In vivo Evaluation of Fluorescence Induction

Athymic male NMRI *nu/nu* mice were purchased from Janvier (Le Genest St.-Isle, France) and were treated according to the ethical guidelines prescribed by United Kingdom Coordinating Committee on Cancer Research. The A2780-$p21^{waf1,cip1}$ZsGreen cells were injected s.c. (10^7/200 μL) into the inguinal region of nude mice and caliper-measurable tumors were obtained after 12 days. Subcutaneous. fluorescent tumors could be detected through the skin of nude mice and measured using an automated whole-body imaging system (12). From day 12, mice were treated p.o. once daily for 1, 2, 3, or 4 days with solvent or the indicated dose of MS-275 (10 animals per group). Tumors were evaluated for fluorescence by the automated whole-body imaging system [fluorescent stereomicroscope type Olympus SZX12 equipped with a green fluorescence filter and coupled to a CCD camera type JAI CV-M90 controlled by a software package based on the IMAQ Vision Software from National Instruments (Austin, TX)]. Median and average value of tumor fluorescence

were calculated by locating the tumor by creating a gray-level image followed by calculating a binary image. The light intensity of all pixels within this area was normalized between 0 (black) and 1 (white). Median light intensity of the tumor was normalized for tumor area.

Fluorescence Microscopy

To evaluate the distribution of ZsGreen protein expression, A2780-p21^{waf1,cip1}ZsGreen tumors were excised, mounted in Peel-A-Way molds (Polysciences, Warrington, PA) with optimum cutting temperature (Sakura, Torrance, CA), and then frozen in liquid nitrogen. Cryosections of 10-μm thickness were mounted on glass slides and air-dried for 30 minutes at room temperature. Within 1 hour after drying, ZsGreen fluorescence was evaluated with an Axioplan 2 (Zeiss) equipped with Epiplan-Neofluar objectives and an Axiocam camera. Images taken with the Axiocam camera from peripheral and central areas of tumor sections from control and treated groups were stored as TIF files and imported in LSM-510 software (Zeiss). To enhance visualization of the distribution of the ZsGreen protein, the imported TIF files were viewed as pseudo three-dimensional pixel intensity maps. For three-dimensional colocalization with tumor vasculature, tumors were collected by transcardial perfusion fixation with 4% paraformaldehyde. Actin and endothelium of blood vessels were visualized by Bodipy 558/568 phalloidin staining and CD-31 (Cy3) immunofluorescent labeling, respectively. Mounted samples were observed with the LSM510 laser scanning microscope.

In vivo Antitumoral Studies

MS-275 was synthesized in-house and formulated at 1 mg/mL in 20% hydroxypropyl-β-cyclodextrin (final pH 8.5) as an injectable solution. A2780-p21^{waf1,cip1}ZsGreen cells were injected s.c. (10^7/200 μL) into the inguinal region of nude mice (athymic male NMRI *nu/nu* mice; Janvier). From day 4, mice were dosed p.o. daily during 35 days (q.d. × 35, p.o.) with MS-275 (10 animals per group, 0.5 mL/mouse). Tumor size was measured with a caliper. Tumor volume was determined by the formula $(a^2 \times b) / 2$, in which a represents the width and b the length.

Results

p21^{waf1,cip1}ZsGreen Reporter Gene Model Predicts the Biological Effect of Histone Deacetylase Inhibitors in Human A2780 Ovarian Cancer Cells

To establish a model enabling real-time visualization of p21^{waf1,cip1} gene transcription, human A2780 ovarian carcinoma cells were stably transfected with a p21^{waf1,cip1} promoter fragment (−1,300 to +88 bp) regulating the expression of ZsGreen fluorescent protein (see Materials and Methods). This promoter region contains key *cis*-acting elements that are required for p21^{waf1,cip1} regulation, including Sp1 sites that mediate its activation by HDAC inhibitors (13, 14).

To validate this engineered cell model, ZsGreen protein expression, and therefore fluorescence signal, needs to reflect the regulation of endogenous p21^{waf1,cip1} in cell-based assays. To study p21^{waf1,cip1} transcriptional regulation, we employed HDAC inhibition, which results in derepression of the p21^{waf1,cip1} promoter, thereby causing cycle arrest (15). As illustrated in Fig. 1, the majority of the A2780-p21^{waf1,cip1}ZsGreen cell population has a low basal fluorescence (i.e., below 10^2 relative fluorescence units). The HDAC inhibitor trichostatin A strongly increased median fluorescence to $>10^3$ relative fluorescence units. To determine to what extent induction of fluorescence predicts the antiproliferative activity, a number of HDAC inhibitors that are currently in phase I and II clinical trials were evaluated [i.e., MS-275 (Berlex/Schering, Berlin, Germany), suberoylanilide hydroxamic acid (SAHA; Merck, Darmstadt, Germany), and LAQ-824 (Novartis, Basel, Switzerland)]. A2780-p21^{waf1,cip1}ZsGreen ovarian carcinoma cells were treated with increasing concentrations of HDAC inhibitors as indicated in Materials and Methods. As shown in Fig. 2A, SAHA and MS-275 induced fluorescence in A2780-p21^{waf1,cip1}ZsGreen cells by 3.6- and 4.3-fold, respectively, at concentrations ranging from 3 to 10 μmol/L, whereas LAQ-824 and trichostatin A were more potent and induced fluorescence 5.5- and 5.2-fold at 0.3 and 1 μmol/L, respectively. This closely reflected the endogenous p21^{waf1,cip1} protein induction by these agents in A2780-p21^{waf1,cip1}ZsGreen cells (Fig. 2B). Again, LAQ-824 and trichostatin A were most potent at 0.3 and 1 μmol/L, respectively, and induced p21^{waf1,cip1} protein levels to a comparable extent as the observed increase in ZsGreen fluorescence (5.5- and 5.7-fold, respectively). SAHA and MS-275 maximally induced endogenous p21^{waf1,cip1} protein expression at 10 μmol/L (4.1- and 6.1-fold, respectively). Similar induction of endogenous p21^{waf1,cip1} protein expression was observed in parental nontransfected A2780 cells (data not shown). The decrease in fluorescence and

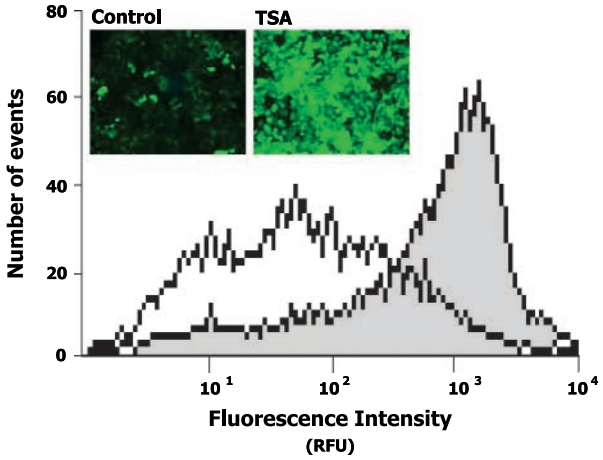

Figure 1. Induction of fluorescence in A2780-p21^{waf,cip1}ZsGreen cells treated by trichostatin A. Human A2780-p21^{waf1,cip1}ZsGreen ovarian tumor cells were incubated for 24 h with 100 nmol/L of trichostatin A (*TSA*). ZsGreen protein production was monitored by fluorescence-activated cell sorting analysis. The autofluorescence peak of the parental A2780 cell line was located between 1 and 10 relative fluorescence units. *Insets,* trichostatin A – induced fluorescence monitored by fluorescent microscope.

$p21^{waf1,cip1}$ protein levels at higher doses was due to cell death. The potency of these agents *vis-à-vis* $p21^{waf1,cip1}$ induction was paralleled by their antiproliferative activity as illustrated in Fig. 2C. Cell proliferation after 4 days was inhibited with IC_{50} values of 4.2 and 3.4 μmol/L for SAHA and MS-275, respectively, which is a similar potency at which an induction of $p21^{waf1,cip1}$ and ZsGreen protein expression was observed after 24 hours. LAQ-824 and trichostatin A inhibited cell proliferation at 0.15 and 0.21 μmol/L (IC_{50}), respectively, whereas ZsGreen protein was induced at 0.3 and 1 μmol/L, respectively. Summarized, these data reveal that fluorescence induction in A2780-$p21^{waf1,cip1}$ZsGreen cells predicts the antiproliferative potency of HDAC inhibitors in cell-based assays.

HDAC Inhibitors Induce Fluorescence in A2780-$p21^{waf1,cip1}$ZsGreen Xenografts in Nude Mice

To investigate whether the $p21^{waf1,cip1}$ZsGreen model could be used to monitor the biological effect of HDAC inhibitors in tumor-bearing mice, studies were done with MS-275. Previous work had shown that MS-275 inhibits A2780-$p21^{waf1,cip1}$ZsGreen tumor growth when cells were grafted s.c. in immunodeficient mice (data not shown). In those studies, mice were treated p.o. with increasing doses of MS-275 once daily for 21 days starting 4 days after injection of cells. At the maximum tolerated dose (20 mpk), tumor growth was inhibited by 83% whereas treatment at 10 mpk resulted in 58% inhibition. Tumor growth inhibition was statistically significant starting on day 14 at both doses, and on day 24 the inhibition of tumor growth at 20 mpk was significantly higher compared with 10 mpk ($P < 0.05$). At 5 mpk, tumor inhibition on day 24 was marginal (31% inhibition; $P = 0.08$, one sided), whereas 2.5 mpk was an inactive dose.

As shown in Fig. 3, MS-275 at biologically active nontoxic doses (i.e., 5, 10, and 20 mpk) clearly induced tumor fluorescence *in vivo* (Fig. 3A). Time course analysis of this induction using automated whole-body imaging of tumor-bearing living animals revealed that a significant induction of fluorescence in the tumor could be detected already after one single administration of MS-275 (Fig. 3B). Dosing at 5, 10, and 20 mpk resulted in a significant increase ($P < 0.05$) in median fluorescence from 0.25 to 0.57, 0.63, and 0.75 absorbance units, respectively. Median fluorescence intensity did not alter at the 5- and 10-mpk dose when treating the mice for 2 or 3 subsequent days. In contrast, at the most active dose (20 mpk), a strong increase in the extent of fluorescence was observed when comparing dosing once (0.75 absorbance unit) with dosing for 2 and 3 days (Fig. 3C, 1.01 and 2.44 absorbance units, respectively). The observed increased $p21^{waf1,cip1}$ promoter activity, when comparing dosing once to dosing for 3 consecutive days, was statistically significant with the Wilcoxon-Mann-Whitney test ($P < 0.05$). These data illustrate that whole-body imaging allows the monitoring of biological responses in the tumor as a function of time. Because a significant response was observed at biologically active (antitumor) doses only (i.e., not at 2.5 mpk; Fig. 3B) and the extent of the response paralleled the known antitumor efficacy of MS-275, this suggested that the $p21^{waf1,cip1}$ZsGreen tumor model can be used to evaluate HDAC inhibitor activity *in vivo* in a short time frame (a few days compared with a few weeks for classic antitumor studies).

When doing long-term *in vivo* studies with antitumor agents, a large variation in the biological response of individual mice is generally observed, requiring the use of large numbers of animals. Because significant variability was also found in the short-term induction of $p21^{waf1,cip1}$-ZsGreen, we sought to investigate whether ZsGreen fluorescence correlated with tumor growth for individual mice. As illustrated in Fig. 4, mice showing high tumor fluorescence also had a relatively low final tumor weight, whereas poor responders (e.g., in the 10- and 15-mpk treatment groups) had higher final tumor weights. In summary, this shows that the $p21^{waf1,cip1}$-ZsGreen fluorescence induction in tumors predicts the extent of response to the treatment with the HDAC inhibitor MS-275 in individual mice.

Localized Response to HDAC Inhibitors within A2780 Tumor Tissue *In vivo*

In addition to predicting long-term antitumor activity, the $p21^{waf1,cip1}$ZsGreen model may also be of value to study the distribution of the biological response within the tumor tissue. To evaluate the tissue distribution of the response to MS-275, a more detailed analysis of the fluorescent signal distribution pattern was done using

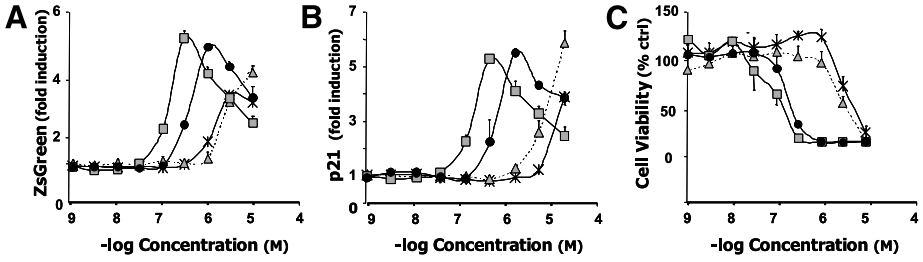

Figure 2. Induction of fluorescence in A2780-$p21^{waf,cip1}$ZsGreen cells predicts biological effect of histone deacetylase inhibitors *in vitro*. Human A2780-$p21^{waf1,cip1}$ZsGreen ovarian tumor cells were treated for 24 h with either the vehicle (0.1% DMSO) or the indicated concentrations of various HDAC inhibitors [SAHA (×), MS-275 (▲), LAQ-824 (■), and trichostatin A (●)]. **A,** dose-dependent induction of fluorescence signal. **B,** dose-dependent induction of $p21^{waf1,cip1}$ protein expression as measured with a p21 ELISA. **C,** dose-dependent inhibition of cell proliferation after 4 d of incubation. *Points,* cell viability expressed as average percent of control for three independent experiments; *bars,* SD.

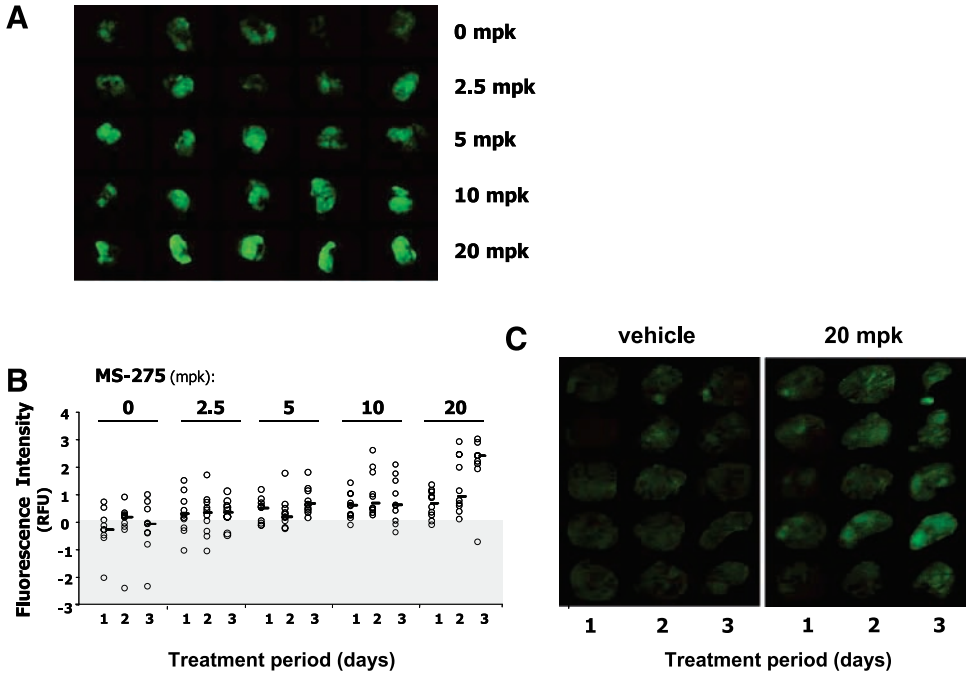

Figure 3. HDAC inhibitor MS-275 induces fluorescence in A2780-p21^{waf1,cip1}ZsGreen xenografts in nude mice. Human A2780-p21^{waf1,cip1}-ZsGreen ovarian tumors cells were injected s.c. into the inguinal region of male athymic *nu/nu* CD-1 mice. When palpable tumors were obtained, mice were treated p.o. once daily for 3 d (q.d. × 3, p.o.) with the indicated dose of MS-275 or vehicle (20% hydroxypropyl-β-cyclodextrin). Tumors were evaluated for fluorescence every day as described in Materials and Methods. **A,** fluorescent signal measured in dissected tumors collected 24 h following the last treatment for five individual mice. **B,** dose- and time-dependent increase in fluorescence using whole-body imaging analysis for individual tumors (10 mice per group). *Columns,* median values. **C,** noninvasive real-time fluorescence using whole-body imaging. Tumors shown are those closest to the median of the group (**B**).

fluorescence analysis of tumor cryosections. A distinct difference in expression of ZsGreen was observed. Fluorescence was much stronger in treated tumors than in controls (Fig. 5). On control samples, only a few areas of high fluorescence intensity were observed (Fig. 5A and C). In treated tumors, ZsGreen-fluorescence was not uniform throughout the tissue. Generally, focal spots of high fluorescence were surrounded by areas with weaker intensity. The areas of these high intensity spots contained from a few cells to hundreds of cells and were found not to colocalize with tumor vasculature. Analysis of sections stained for β-actin showed that ZsGreen-labeling was localized in the cytoplasm of the tumor cells (Supplementary Fig. S6).[5] There was no difference in fluorescence between the peripheral and central parts of the tumor (Fig. 5B and D), indicating exposure of the drug and/or a biological response throughout the entire tumor.

Discussion

Technologies that allow real-time molecular imaging of gene expression offer the potential for increasing our understanding of disease biology, evaluating disease treatment *in vivo*, and visualizing the effects of drugs at the cellular level in living animals (16). This report shows that A2780-p21^{waf1,cip1}ZsGreen ovarian xenografts allow noninvasive real-time assessment of the regulation of gene expression in living tumor-bearing mice. ZsGreen fluorescence fully parallels regulation of the endogenous p21^{waf1,cip1} protein, and induction of fluorescence *in vivo* accurately predicted the long-term antitumoral activity of HDAC inhibitors in individual mice. Because p21^{waf1,cip1} is commonly regulated by anticancer agents, such as azacytidine, taxanes, anthracyclins, and cisplatin, this model is not limited to the evaluation of HDAC inhibitors but has broader application. Finally, induction of p21^{waf1,cip1} promoter activity *in vivo* was observed in both the central and peripheral regions of the treated tumors, indicating a biological response in the entire tumor.

Although whole-body imaging of highly fluorescent xenografts is commonly used to monitor tumor growth over time (17), real-time monitoring of gene regulation *in vivo* in response to pharmaceutical agents represents an emerging field. Noninvasive *in vivo* imaging has been described for a number of signal transduction processes such as protease activity, protein-protein interactions, and protein degradation (18–21). For example, Bremer and Tung (18) described visualization of the inhibition of matrix metalloproteinase protease activity in intact tumor-bearing mice with Prinomastat (AG3340). This involved the delivery of fluorescent probes of which the properties change after being bound or cleaved, such as in the case of fluorescence recovery after photobleaching (22) and imaging using autoquenched near-IR fluorescence (23). *In vivo* analysis of protein degradation was shown by Luker et al. (20) by monitoring overall proteasome activity by imaging turnover of a labile luciferase protein, whereas Zhang et al. (21) monitored cyclin-dependent kinase-2 activity *in vivo* by imaging the turnover of a p27-luciferase fusion protein. Recently, Qian et al. (24) described reactivation of the retinoic acid receptor β2 promoter by MS-275 and retinoids in PC3 prostate xenografts using bioluminescence. However, in all these studies, a link was not established between the signal transduction response and final therapeutic outcome.

[5] Supplementary material for this article is available at Molecular Cancer Therapeutics Online (http://mct.aacrjournals.org/).

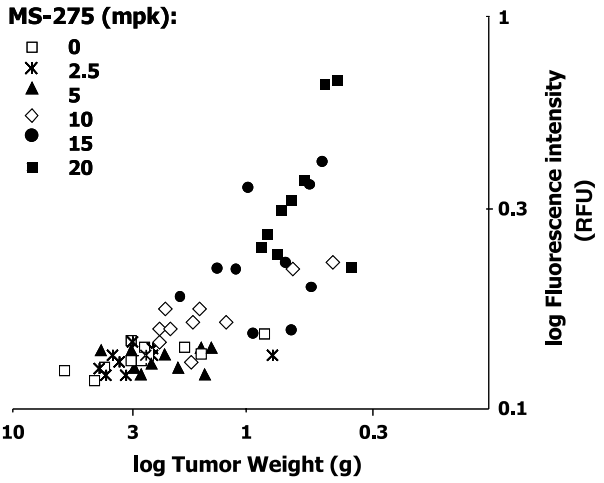

Figure 4. Induction of fluorescence in p21^{waf,cip1} promoter- ZsGreen tumor model predicts antitumor effect of MS-275 in nude mice. Human A2780-p21^{waf1,cip1}ZsGreen ovarian tumor cells were injected s.c. into the inguinal region of male athymic *nu/nu* CD-1 mice, and from day 4, animals were treated p.o. once daily with either vehicle (control group, 20% hydroxypropyl-β-cyclodextrin) or HDAC inhibitor, MS-275, at the indicated doses. Tumor weight and fluorescence of individual dissected tumors were evaluated on day 28 using the automated whole-body imaging system. Linear regression showed a correlation coefficient of $r = 0.79$.

To monitor real-time gene expression regulation *in vivo*, fluorescent protein expression was used as a reporter because of its compatibility with unanesthesized animals and because it does not require the delivery of a substrate to the tumor before imaging. This second aspect is important when studying *in vivo* gene responses to pharmaceutical agents because a substrate may nonspecifically modulate gene expression or might interfere with the pharmacokinetics or pharmacodynamics of the investigational drug (16). This issue is illustrated by the work of Doubrovin et al. (25). The enzyme herpes simplex virus-1 thymidine kinase was expressed under the control of a p53-responsive element, enabling positron emission tomography imaging of gene expression after administration of the thymidine kinase substrate [^{124}I]-2′-fluoro-2′-deoxy-1β-D-arabinofuranosyl-5-iodouracil. Although a significant increase in radioactivity was observed in [*N*,*N*′-bis(2-chloroethyl)-*N*-nitrosourea]–treated rats as compared with control animals, interpretation of these data was hampered by a nonspecific response to [*N*,*N*′-bis(2-chloroethyl)-*N*-nitrosourea] in nontransgene tissue. This was linked to a changed pharmacokinetic profile of the [^{124}I]-2′-fluoro-2′-deoxy-1β-D-arabinofuranosyl-5-iodouracil substrate, presumably due to the nonspecific toxic affects of [*N*,*N*′-bis(2-chloroethyl)-*N*-nitrosourea]. In addition to the risk of changing pharmacokinetic properties when coadministrating both an activator of signal transduction and a positron emission tomography substrate, the radioactive substrates needed for positron emission tomography technology may potentially also induce DNA damage/stress pathways and thereby activate p53 signaling. These data clearly illustrate the importance of nonsubstrate dependent assays when evaluating antitumoral therapeutic agents. These drawbacks were circumvented by engineering the stable A2780 ovarian carcinoma cell line in which the p21^{waf1,cip1} promoter (−1,300 to +88 bp) regulates the expression of ZsGreen fluorescence.

In this article, we have used HDAC inhibitors to induce the expression of the cyclin-dependent kinase inhibitor p21^{waf1,cip1}. A causal relationship between this p21^{waf1,cip1} up-regulation and the antiproliferative effects of HDAC inhibitors has previously been established by studies showing that p21^{waf1,cip1}-deficient HCT-116 human colon carcinoma cells have increased resistance to these agents (15, 26). HDAC inhibitors activate p21^{waf1,cip1} gene expression by dissociating the HDAC repressor complex from the

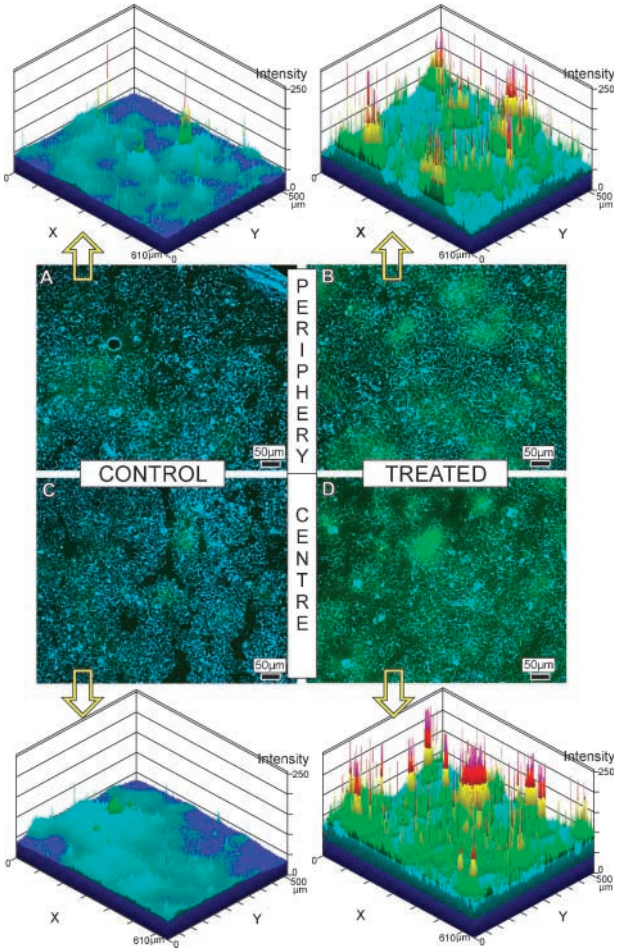

Figure 5. Localization of biological response to MS-275 in A2780-p21^{waf1,cip1}ZsGreen tumors. Distribution of ZsGreen fluorescent signal in unfixed dry cryosections from control nude mice (**A** and **C**) or animals treated with MS-275 at 20 mg/kg (q.d., p.o.) for 4 d (**B** and **D**). To reveal the distribution of ZsGreen fluorescence in the tissue, fluorescent images (*green*) were taken of both the peripheral (**A** and **B**) and central (**C** and **D**) areas of the tumors and were merged with images taken with reflected light microscopy. Reflected light (*light blue*) allows detection of cellular borders and interstitial tissue. *Top* and *bottom,* pseudo three-dimensional pixel intensity maps of the ZsGreen fluorescent signal from each image.

transcriptional activator Sp1, which drives $p21^{waf1,cip1}$ transcriptional activity. ZsGreen fluorescence was found to fully parallel the regulation of the endogenous $p21^{waf1,cip1}$ protein by a panel of HDAC inhibitors *in vitro*. This is in agreement with other reports showing that trichostatin A, MS-275, and SAHA induce transactivation of the murine $p21^{waf1,cip1}$ promoter through the Sp1 sites located within the −166 to +40 bp region relative to the TATA box (12, 14), a region contained within our $p21^{waf1,cip1}$ −1,300 to +88 bp promoter construct. In agreement with the key role of $p21^{waf1,cip1}$ in the antitumor effects of many neoplastic agents, induction of $p21^{waf1,cip1}$ promoter–driven fluorescence *in vivo* was found to properly predict the long-term antitumor activity of anticancer agents. Furthermore, kinetic analysis of the fluorescence after several days of dosing indicated accumulation of response after 3 days of dosing for MS-275 at 20 mpk, but not at 10 mpk. This is in agreement with the higher antitumor activity of this agent at 20 mpk. Such a cumulative effect at higher doses may point to accumulation of the compound in tumor tissue over time or changed pharmacokinetic behavior of the agent after repeated dosing. Although the pharmacokinetic profile of MS-275 in mice is not known, early data from clinical trials in human show a long half-life for this agent (29.9 hours) and an increase in exposure at the second dose in four of six patients (27). Interestingly, the fluorescence response was found to be predictive for tumor growth in individual mice. Typically, the response of individual animals to neoplastic agents shows a high variability, which is why large numbers of animals are used for each dose group in this kind of study. Pharmacokinetic analysis showed comparable levels of drug in the tumor tissue between individual animals. Therefore, our data indicate that the high interindividual variation in tumor growth inhibition is dictated by the absence of the biological response to these agents and is not due to lack of activation of HDAC regulated genes.

In summary, our data indicate that the $p21^{waf1,cip1}$ promoter fluorescent xenografts provide a powerful tool that allows rapid assessment of *in vivo* antitumoral activity. This facilitates earlier evaluation of the compounds in the drug discovery process without the need for time- and reagent-consuming pharmacokinetic/pharmacodynamic studies, thereby accelerating significantly the discovery and development of novel antitumor agents.

Acknowledgments

We thank Dr. Jorge Vialard for critical reading of the manuscript.

References

1. Kaelin WG, Jr. Choosing anticancer drug targets in the postgenomic era. J Clin Invest 1999;104:1503 – 6.

2. Fisher DE. Turning p53 on or off: either way may treat cancer. Drug Resist Updat 2000;3:77 – 9.

3. Bunz F, Hwang PM, Torrance C, et al. Disruption of p53 in human cancer cells alters the responses to therapeutic agents. J Clin Invest 1999; 104:263 – 9.

4. Bunz F, Dutriaux A, Lengauer C, et al. Requirement for p53 and p21 to sustain G_2 arrest after DNA damage. Science 1998;282:1497 – 501.

5. Deng C, Zhang P, Harper JW, Elledge SJ, Leder P. Mice lacking $p21^{CIP1/WAF1}$ undergo normal development, but are defective in G_1 checkpoint control. Cell 1995;82:675 – 84.

6. Cheng M, Olivier P, Diehl JA, et al. The $p21^{Cip1}$ and $p27^{Kip1}$ CDK ''inhibitors'' are essential activators of cyclin D-dependent kinases in murine fibroblasts. EMBO J 1999;18:1571 – 83.

7. Martín-Caballero J, Flores JM, García-Palencia P, Serrano M. Tumor susceptibility of $p21^{Waf1/Cip1}$-deficient mice. Cancer Res 2001;61: 6234 – 8.

8. Dotto GP. $p21^{WAF1/Cip1}$: more than a break to the cell cycle? Biochim Biophys Acta 2000;1471:M43 – 56.

9. Lagger G, Doetzlhofer A, Schuettengruber B. The tumor suppressor p53 and histone deacetylase 1 are antagonistic regulators of the cyclin-dependent kinase inhibitor p21/WAF1/CIP1 gene. Mol Cell Biol 2003;23: 2669 – 79.

10. Cress WD, Seto E. Histone deacetylase, transcriptional control, and cancer. J Cell Physiol 2000;184:1 – 16.

11. Marks PA, Rifkind RA, Richon VM, Breslow R, Miller T, Kelly WK. Histone deacetylase and cancer: causes and therapies. Nat Rev 2001;1: 194 – 202.

12. Bakker A, Floren W, Voeten J, et al. Automation of whole body imaging of green fluorescent protein-expressing tumors in living animals. GIT Imaging & Microscopy 2001;3:52 – 4.

13. Xiao H, Hasegawa T, Isobe K. Both Sp1 and Sp3 are responsible for p21waf1 promoter activity induced by histone deacetylase inhibitor in NIH3T3 cells. J Cell Biochem 1999;73:291 – 302.

14. Huang L, Sowa Y, Sakai T, Pardee AB. Activation of the p21WAF1/CIP1 promoter independent of p53 by the histone deacetylase inhibitor suberoylanilide hydroxamic acid (SAHA) through the Sp1 sites. Oncogene 2000;19:5712 – 9.

15. Archer SY, Meng S, Shei A, Hodin RA. $p21^{WAF1}$ is required for butyrate-mediated growth inhibition of human colon cancer cells. Proc Natl Acad Sci U S A 1998;95:6791 – 6.

16. Massoud TF, Gambhir SS. Molecular imaging in living subjects: seeing fundamental biological processes in a new light. Genes Dev 2003;17: 545 – 80.

17. Bouvet M, Wang J, Nardin SR, et al. Real-time optical imaging of primary tumor growth and multiple metastatic events in a pancreatic cancer orthotopic model. Cancer Res 2002;62:1534 – 40.

18. Bremer C, Tung C-H, Weissleder R. *In vivo* molecular target assessment of matrix metalloproteinase inhibition. Nat Med 2001;7: 743 – 8.

19. Paulmurugan R, Massoud TF, Huang J, Gambhir SS. Molecular imaging of drug-modulated protein-protein interactions in living subjects. Cancer Res 2004;64:2113 – 9.

20. Luker GD, Pica CM, Song J, Luker KE, Piwnica-Worms D. Imaging 26S proteasome activity and inhibition in living mice. Nat Med 2003;9: 969 – 73.

21. Zhang G-J, Safran M, Wei W, et al. Bioluminescent imaging of cdk2 inhibition *in vivo*. Nat Med 2004;10:643 – 8.

22. Berk DA, Yuan F, Leunig M, Jain RK. Direct *in vivo* measurement of targeted binding in a human tumor xenograft. Proc Natl Acad Sci U S A 1997;94:1785 – 90.

23. Weissleder R, Tung C-H, Mahmood U, Bodganov A, Jr. *In vivo* imaging of tumors with protease-activated near-infrared fluorescent probes. Nat Biotechnol 1999;17:375 – 8.

24. Qian DZ, Ren M, Wei Y, et al. *In vivo* imaging of retinoic acid receptor β2 transcriptional activation by the histone deacetylase inhibitor MS-275 in retinoid-resistant prostate cancer cells. Prostate 2005;64: 20 – 8.

25. Doubrovin M, Ponomarev V, Beresten T, et al. Imaging transcriptional regulation of p53-dependent genes with positron emission tomography *in vivo*. Proc Natl Acad Sci U S A 2001;98:9300 – 5.

26. Kim YB, Ki SW, Yoshida M, Horinouchi S. Mechanism of cell cycle arrest caused by histone deacetylase inhibitors in human carcinoma cells. J Antibiot 2000;53:1191 – 200.

27. Gojo I, Karp JE, Mann D, et al. Phase I study of histone deactylase inhibitor (HDI) MS-275 in adults with refractory or relapsed hematologic malignancies [abstract no 2198]. Proc Am Soc Hem 2002.

Molecular Cancer Therapeutics

Real-time gene expression analysis in human xenografts for evaluation of histone deacetylase inhibitors

Ann Beliën, Stefanie De Schepper, Wim Floren, et al.

Mol Cancer Ther 2006;5:2317-2323.